Hindawi Publishing Corporation
International Journal of Optics
Volume 2011, Article ID 215404, 7 pages
doi:10.1155/2011/215404

Research Article

Stress Analysis in Glass Artwork

João M. P. Coelho,[1] Catarina Silva,[1] and Teresa Almeida[2,3,4]

[1] *Laboratório de Óptica Lasers e Sistemas, Departamento de Física, Faculdade de Ciências da Universidade de Lisboa, Campus do Lumiar, Estrada do Paço do Lumiar, 22, Building D, 1649-038 Lisbon, Portugal*
[2] *Vidro e Cerâmica para as Artes (VICARTE), Faculdade de Ciências e Tecnologia, Universidade Nova de Lisboa, 2829-516 Caparica, Portugal*
[3] *Departamento de Pintura, Faculdade de Belas Artes da Universidade do Porto, Avenida Rodrigues de Freitas, 265, 4049-021 Porto, Portugal*
[4] *Departamento de Comunicação e Arte, Universidade de Aveiro, Campos Universitário de Santiago, 3810-193 Aveiro, Portugal*

Correspondence should be addressed to João M. P. Coelho, joao.coelho@fc.ul.pt

Received 24 September 2010; Accepted 11 March 2011

Academic Editor: Chenggen Quan

A simple method for determining the stress fields in transparent glass artwork pieces is presented. The proposed method is based on the principles of photoelasticity combining imaging and quantitative measures with an image processing algorithm. The main goal was to develop a methodology to help glass artists to determine the ability of their work to resist the thermal shocks by giving them a hazard map based on the stress map of the glass piece.

1. Introduction

Glass artwork has long followed the human search by exquisite artistic pieces. Shapes, colors, and their ability to always "change" with different illumination make these pieces desirable to many artists. However, working with glass also presents some risk since thermal stress is always present when dealing with glass materials in spite of the techniques used, namely glass blowing, casting, or *pâte de verre* (a form of kiln casting [1]).

For these reasons, the measurement of residual stresses should become a fundamental element in quality control operation of the glass artwork. In this scope, the photoelastic stress analysis is one of several methods used to estimate the distribution stress in glass materials [2–7].

Residual stress is an intrinsic tension or compression which exists in a material without an external load being applied. In glass, the so-called permanent residual stress is induced in the primary manufacturing process and the potential resistance to thermal stresses accessed through the material's Young Modulus, E [8]. These stresses might be relieved through annealing or subsequently added in secondary thermal processing operations to induce desired mechanical characteristics.

A proper annealing of the glass pieces is very important to eliminate the inside stresses. The methodology used by the artists is somewhat empirical, and knowing the transition temperature and the strain point would be very important. Depending on the glass type, shape, and thickness of the art pieces different firing schedules are being used by several artists in order to achieve the best results to avoid stress or fractures. Tables with annealing cycles can be found in the literature [9–11].

When there is equilibrium between the tensile and compressive stresses, the glass is said to be stable. An imbalance in residual stresses can cause unexpected weakness or spontaneous fracture. In either case, to know the stress distribution in a glass volume is of outmost importance. Several techniques are being used by the industry, artisans, artists, and scientists. However, the large majority relies on the concepts of photoelasticity.

Photoelasticity can be defined as the property exhibited by some transparent solids, whereby they become doubly refractive, or "birefringent," when subjected to stress. When

Figure 1: Picture of the polariscope used in this work.

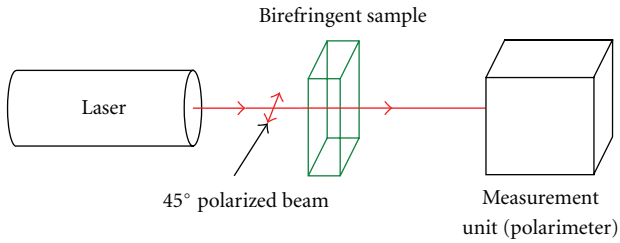

Figure 2: Phase-difference measurement setup based on a polarimeter.

polarized light passes through a stressed material, the light separates into two wavefronts travelling at different velocities, each oriented parallel to a direction of principal stress (σ_1, σ_2) in the material, but perpendicular to each other.

Birefringence results in the stressed material having two different indices of refraction (n_1, n_2). In most materials, the index of refraction remains constant; however, in glass and plastics, its value varies as a function of the stress applied. This gave rise to the stress-optic, or Brewster's, law:

$$(n_1 - n_2) = C_B(\sigma_1 - \sigma_2), \tag{1}$$

C_B being the stress-optical constant or Brewster constant. Therefore, this law establishes that birefringence is directly proportional to the difference of principal stresses, which is equal to the difference between the two indices of refraction, $n_1 - n_2$, exhibited by a stressed material. Therefore, birefringence can be calculated by having $\Delta n = n_1 - n_2$.

The phase difference between the two light vectors travelling through the material with different velocities (fast, slow) is known as retardation, δ. The retardation value divided by the material's thickness, h, is proportional to the difference between the two indices of refraction, that is,

$$\Delta n = \frac{\delta}{h}. \tag{2}$$

Combining (1) and (2), the stress equation is obtained:

$$\Delta\sigma = \sigma = \frac{\delta}{h \cdot C_B}. \tag{3}$$

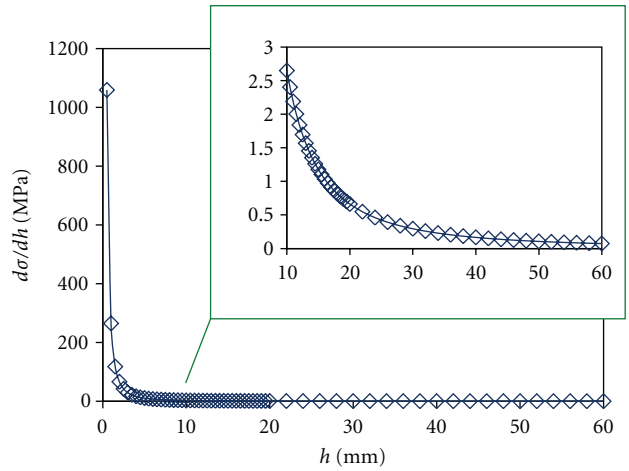

Figure 3: Influence of sample's thickness on the stress calculus.

In the glass-related industry, polariscopes are the main instrument in the stress analysis of transparent pieces. These are essential instrument for the visualizing of strain patterns in most transparent materials. When a specimen exhibiting stress is illuminated with polarized light from a polariscope, a pattern of various colors appear which are directly proportional to the stresses within the material [12]. However, it only allows obtaining the qualitative evolution of stress in an object and cannot provide quantitative information of the phase retardation [2]. Usually, two polarizer filters allow the user to see compressive stresses as red-related areas while tensile stresses as bluish areas.

There are different methods to measure the state of polarization of a light beam [13–15]. The polarimeter used in this work is based on the rotating quarter waveplate technique [6, 16]. This sensor consists of a rotating quarter waveplate, a fixed linear polarizer, and a photodiode. Then, the polarizer only transmits the portion of light which is parallel to the transmission axis. The photodiode acts as a powermeter and allows mapping the input beam's polarization as the quarter waveplate rotates. Using this device, for linear polarized light, at 45° polarized, the retardance can be obtained from the phase difference $\Delta\phi$ by

$$\delta = \frac{\lambda\Delta\phi}{2\pi}, \tag{4}$$

and (3) can be expressed as

$$\sigma = \frac{\lambda\Delta\phi}{2\pi h C_B}. \tag{5}$$

In this work, the authors present a method to make use of both polariscope images and polarimeter data to obtain the full stress map of artistic pieces. This method relies on the photoelastic theory and image processing algorithms.

2. Methodology

The method proposed is based on the correlation between polariscope qualitative stress images and quantitative polariscope information. Using a common polariscope (Figure 1),

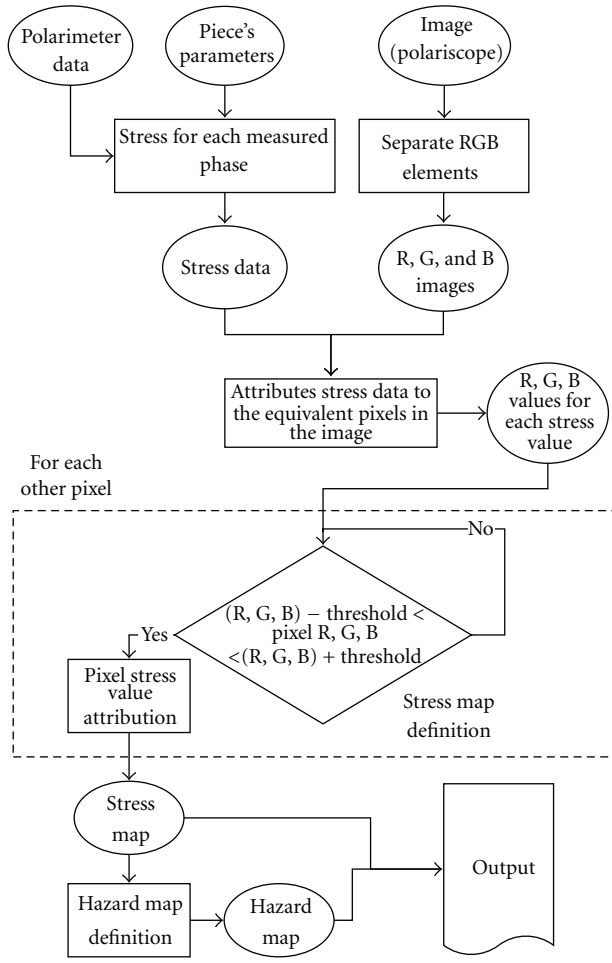

Figure 4: Flow diagram of the algorithm developed for stress and hazard maps generation.

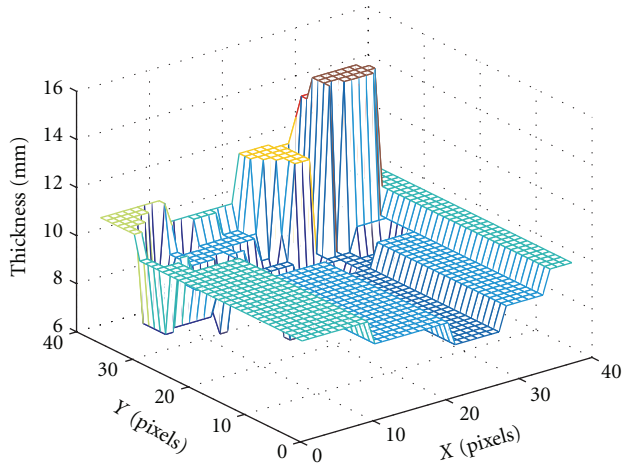

Figure 5: Thickness map for the test object "Vitral 2."

a digital color camera (Sony DSV-V1) captured images from the color pattern. These images were then recorded as JPEG images.

In order to provide the necessary quantitative stress data, a linear polarimeter (PAX 5710) was used to measure the phase difference, with which the retardation values were estimated, and consequently, the stress value. A laser source, a polarizer, a rotation stage to hold the sample, and the PAX 5710 polarimeter were necessary for this measurement setup. The polarimeter was illuminated with a monochromatic laser source: a He-Ne laser, emitting a beam of 632.8 nm wavelength monochromatic polarized light (1000 : 1), with its polarization axis oriented at 45°. The principle is illustrated in Figure 2.

Of course, artwork pieces do not have constant thickness. In the opposite, their different shapes have as a consequence possible quite drastic changes in that parameter. Two possible approaches can be considered when the method hereby described is applied: (1) to produce a thickness map of the piece under analysis or (2) to consider an average thickness over the area of testing. The first hypothesis requires an "extra" step in the process that, depending on the piece's shape, can be sometimes quite difficult. The second step requires a careful analysis of the effect on the resulting data. In either case, the analysis of the effect of thickness change on

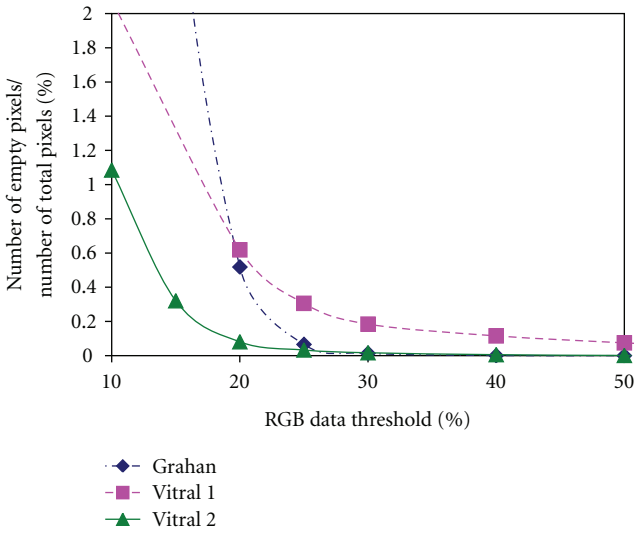

Figure 6: Percentage of empty pixels for different RGB thresholds.

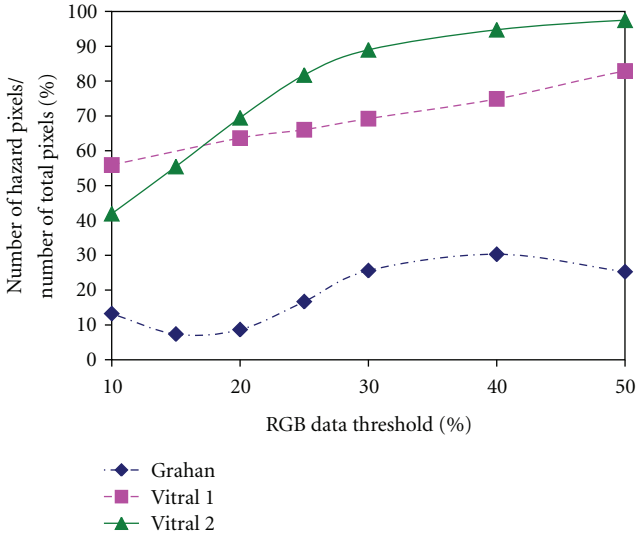

Figure 7: Percentage of hazard pixels for different RGB thresholds.

the stress calculus is required. In order to obtain this information, (5) was derived with respect to h, resulting

$$\frac{\partial}{\partial h}\sigma = -\frac{1}{2}\frac{\lambda \cdot \Delta\phi}{\pi C_B h^2} \tag{6}$$

and typical data for a silicate glass was used (Table 1). Figure 3 shows the behavior of the stress change with sample's thickness. The plot shows that the thinner the sample, the higher its sensitivity to thickness changes which implies that, for high stress values and high thickness, the piece can be considered as having uniform thickness. In such cases, an average value may be considered as a "safe" option.

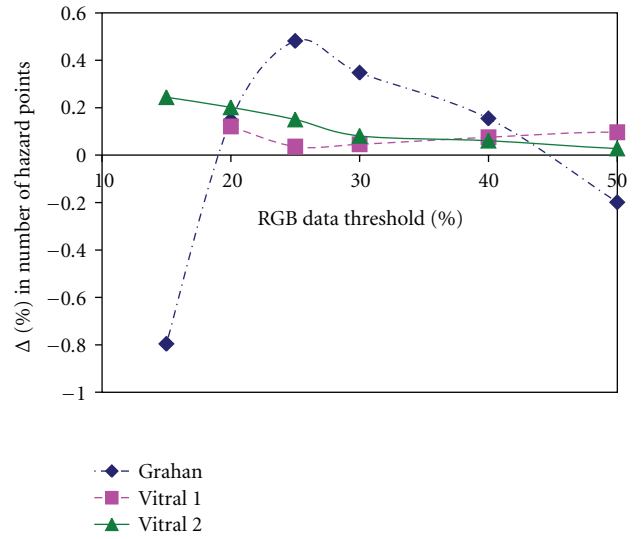

Figure 8: Variation in the percentage of hazard points as the RGB threshold increases.

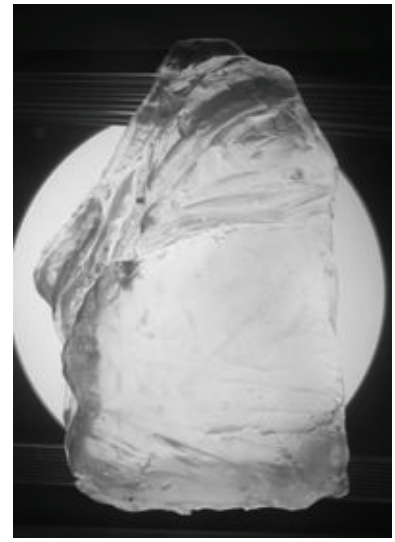

Figure 9: Picture of the artwork (Grahan) analyzed as an example of the method hereby described.

Table 1: Typical parameters used in the study of the thickness influence.

λ [$\times 10^{-9}$ m]	C_B [10^{12} m^2/N]	$\Delta\phi$ [°]
632	3.8	10

3. Image Processing Algorithm

The proposed algorithm has three main steps; the first consists in acquiring the image of the color pattern obtained by a polariscope and its separation into three monochromatic images. The color of each pixel in the image is represented by three components: red, green, and blue (RGB). After reading the RGB value of a given pixel color, in the second step, the color of each pixel is converted to data according

Table 2: Characteristics of the objects tested.

Test object		"Grahan"	"Vitral 1"	"Vitral 2"
Thickness (mm)*		60	10	9.3
Young Modulus (GPa)			92	
C_B (10^{12} m^2/N)			3.8	
Critical Stress	Traction		9.2	
(MPa)	Compression		−92	
Tested area (mm)^2		100 × 100	190 × 180	380 × 370

* Average.

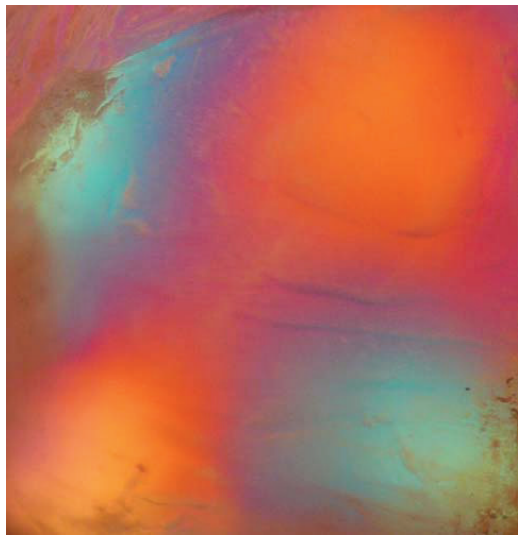

Figure 10: Image of the color patterns obtained by the polariscope.

to information obtained by phase-difference matrix. Then, for each spatial position the algorithm finds the information about the correspondent pixel: color component and phase difference. Assuming that points in the image having the same color have also equal stresses, a cycle attributes a phase-difference value to the pixels in the image with RGB values near those of exact data pixels (according to a specified threshold value). Subsequently, from the phase-difference data, values of the stress are obtained (stress map) and assigned to those positions.

Finally, in the third step, from the stress map, a hazard map is created, indicating zones under critical stress. A pixel value equivalent to white is attributed to zones with low stresses (no-risk pixels) while a pixel value equivalent to black is attributed to higher stresses (hazard pixels), either tensile or compressive. Predefined glass type and user-defined optical stress parameters allow the code to define the critical stresses and to display the distributions of the stress magnitude. These procedures are schematized in Figure 4.

One of the main user-defined parameters is the threshold value, *thRGB*, defined as a percentage of the RGB values equivalent to the experimentally obtained stress values. These values should be chosen by proper calibration procedures or by comparison with other data. In this work, this parameter was analyzed and chosen by relating it with its impact on the stress map and comparing it with previously qualitative data. Future work should address defining a specific calibration procedure.

4. Experimental Results

The described method was tested with several artwork pieces, with different glass compositions. In the scope of this paper, we only considered transparent or mild "non-RGB" (i.e., not highly red, green, or blue) colored pieces.

As mentioned before, the threshold value applied for pixel RGB comparison plays a major role in the process (although not really critical in the overall analysis, as will be explained further on). In order to analyze its impact and choose its values, three artwork pieces were chosen, made with different recipes, and coded as "Grahan," "Vitral 1," and "Vitral 2." Previous qualitative tests demonstrated no real problem with the first of these pieces while the others have demonstrated rather problematic response on other pieces under similar condition. The objects were observed at CRISFORM facilities with a polariscope Sharple Senarcon Strhin. A polarizing film was used to check if the strain in all the glass pieces ("Grahan," "Vitral 1," and "Vitral 2") is in accord with the ASTM protocol C 671-94, F218-95, C 148-95.

As "Grahan" and "Vitral 1" showed no significant change in their thickness, an average value was considered, while a thickness map was produced for "Vitral 2" (Figure 5). The characteristics of the tested objects are present in Table 2.

Since the number of phase measurements is limited ("Grahan": 100; "Vitral 1": 342; "Vitral 2": 1406), one of the analyses was made on the influence of the *thRGB* parameter on the number of empty (no data) values in the final maps. Figure 6 shows the variation in the percentage of empty pixels as *thRGB* changes for the considered test objects. As it can be seen, a threshold between 25% and 30% reduces the percentage of empty data to less than 0.5%. One should note that "Vitral 1" has a large number of empty pixels at the edges of the image, which were not considered in the final analysis.

Another analysis was made on the impact of the *thRGB* parameter on the number of pixels identified as hazard ones. Figure 7 shows the number of determined hazard pixels and Figure 8 the evolution in their percentage as *thRGB* varies. Again, a threshold between 25 and 30% seems to be a proper value to achieve valid results since higher values, in general, do not have a major impact on the analyzed factors.

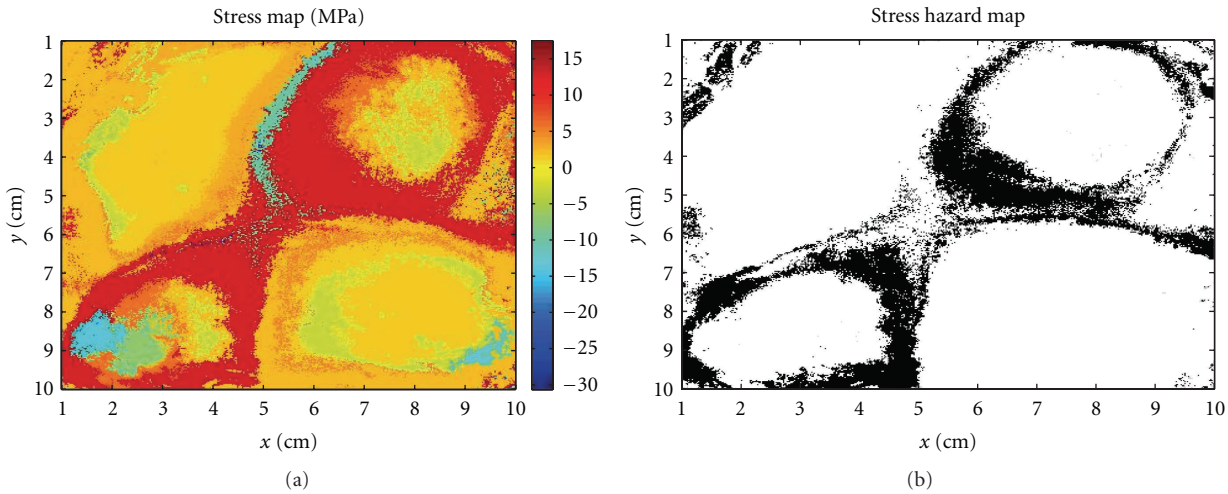

Figure 11: Image processing outputs of (a) the distribution of principal stresses obtained by measuring the phase difference and (b) the stress hazard map. The RGB threshold was chosen to be 30%.

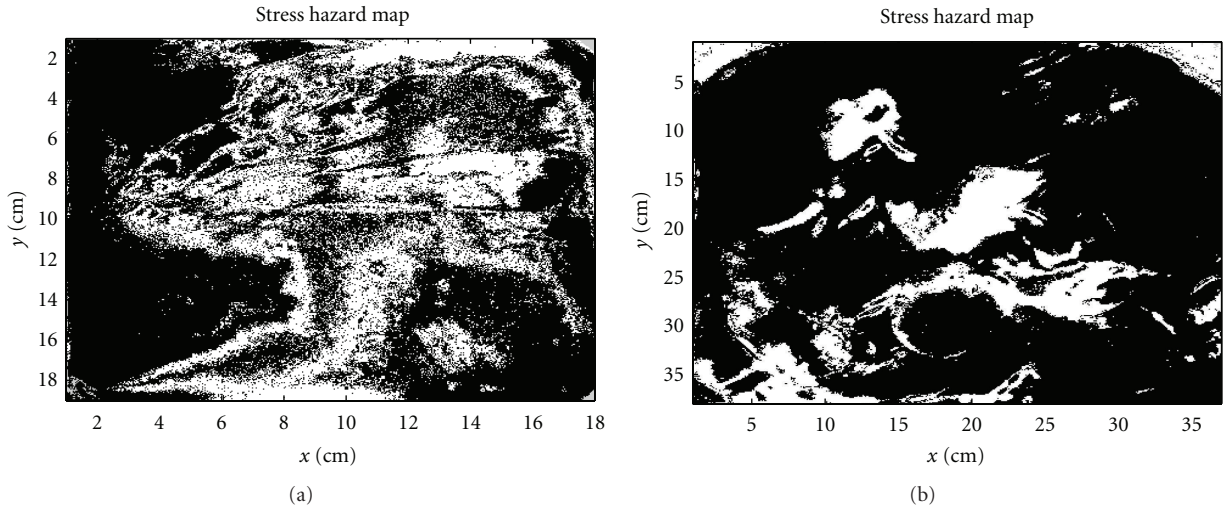

Figure 12: Stress hazard map obtained for (a) "Vitral 1" and (b) "Vitral 2," with RGB threshold of 30%.

Also, after testing the methodology for all the samples, with different *thRGB* values, even if the number of hazard points increases, the conclusions in their analysis remained from thresholds higher than 20%. Of course, hazard areas do not necessarily indicate points were the piece will break but just areas where stresses might lead to it when the piece is subjected to thermal shocks [8].

As an example of the results obtained, we choose the artwork "Grahan," imaged in Figure 9. Its thickness changes only about 2 mm (60 mm average) over the analyzed area, which according to the previous analysis (Figure 3) leads us to consider the average thickness instead of the complete thickness map. Considering the discussion above, we choose to use $thRGB = 0.3$ (30%).

Figure 10 shows the image taken from the polariscope: red represents compressive stresses while blue tensile stresses, as seen through the polariscope red and blue filters. Using the method described above, we measured the phase difference and estimated the phase retardation. Stresses were calculated using the stress-optic relation given in (5).

Figure 11 shows the stress distribution obtained theoretically and the equivalent hazard map, considering that the maximum allowed stress (in modulus) is $\sim 10^{-4}E$ for tensile stress (negative stresses) and $\sim 10^{-3}E$ for compressive stress (positive) [8]. Using these limits, the dark areas in the stress hazard map are potential risk areas while the white areas have no risk. Computation was carried out for a silicate glass with $E = 92$ GPa and $C_B = 3.8 \times 10^{12}$ m^2/N, illuminated with 632.8 nm wavelength HeNe laser radiation.

The technique was also applied to "Vitral 1" and "Vitral 2," and the resulting hazard maps are plotted in Figure 12. As it can be observed, the stress-associated risk is higher for this artwork piece than for "Grahan" piece, and care should be taken regarding its subjection to thermal shocks.

5. Conclusions

A simple method based on the principles of photoelasticity for determining the stresses field in glass materials was developed. By combining imaging and quantitative measures with an image processing algorithm, it was possible to obtain an indication of the stress map over large glass artwork pieces and acquire a hazard map. The impact of thickness variations on the obtained results was also studied.

Although results were consistent with alternative (qualitative) analysis, the authors also verified that a calibration method should be defined in future research on the subject. Nevertheless, this methodology could be a simple and reliable way of an artist to analyze the potential of his work to resist the thermal shocks.

Acknowledgments

The authors would like to acknowledge Mr. Fernando Monteiro from LOLS/FCUL and Marta Ferro of the Universidade de Aveiro, Department of Ceramic and Glass Engineering, for their collaboration in this work. The author T. Almeida would like to be grateful to the Fundação para a Ciência e a Tecnologia (FCT) for financial support (REF: under contract SFRH/BD/30684/2006). Also, the paper was partially supported by FCT Project PTDC/EAT/67354/2006.

References

[1] J. Kervin and J. Kervin, *Pâte de Verre and Kiln Casting of Glass*, Glasswear Studios, Livermore, Calif, USA, 2nd edition, 2000.

[2] T. W. Ng, "Photoelastic stress analysis using an object step-loading method," *Experimental Mechanics*, vol. 37, no. 2, pp. 137–141, 1997.

[3] J. Villa, J. Antonio Quiroga, and E. Pascual, "Determination of isoclinics in photoelasticity with a fast regularized estimator," *Optics and Lasers in Engineering*, vol. 46, no. 3, pp. 236–242, 2008.

[4] J. F. Lin, T. T. Liao, Y. L. Lo, and S. Y. Lee, "The optical linear birefringence measurement using a Zeeman laser," *Optics Communications*, vol. 274, no. 1, pp. 153–158, 2007.

[5] D. W. Fletcher-Holmes and C. C. Hoyt, "Non-intrusive measurement of stress in transparent materials," *Microscopy and Microanalysis*, vol. 12, no. 2, pp. 952–953, 2006.

[6] A. Redner, "Measuring stress in glass production: a key quality control operation," *Glass Production Technology International*, pp. 180–183, 1995.

[7] J. F. Ganghoffer, "Calculation of thermal stresses in glass-ceramic composites," *Mechanics Time-Dependent Materials*, vol. 4, no. 4, pp. 359–379, 2000.

[8] M. Bartener, *The Structure and Mechanical Properties of Inorganic Glass*, Wolters-Noordfoff Editors, Groningen, The Netherlands, 1970.

[9] H. Halem, *Glass Notes: A Reference for the Glass Artist*, Franklin Mills Press, Kent, Ohio, USA, 3rd edition, 2006.

[10] G. Stone, *Firing Schedules for Glass*, Melbourne, Australia, 1st edition, 2000.

[11] K. Cummings, *Techniques of Kiln-Formed Glass*, A&C Black Publishers Limited, London, UK, 1997.

[12] J. M. Feingold, "Stress diagnose it before it ruins your parts," in *Plastics Technology*, Gardner Publications, Inc., 2009, http://www.ptonline.com/articles/200512fa2.html.

[13] R. M. A. Azzam, "Rotating-detector ellipsometer for measurement of the state of polarization of light," *Optics Letters*, vol. 10, no. 9, pp. 427–429, 1985.

[14] E. Hasman, G. Biener, V. Kleiner, and A. Niv, "Spatial Fourier-transform polarimetry by use of space-variant subwavelength gratings," *Optics and Photonics News*, vol. 14, no. 12, p. 34, 2003.

[15] L. A. Ferreira, F. M. Araújo, J. L. Santos, and F. Farahi, "Simultaneous measurement of strain and temperature using interferometrically interrogated fiber Bragg grating sensors," *Optical Engineering*, vol. 39, no. 8, pp. 2226–2234, 2000.

[16] J. Villa, J. A. Quiroga, and J. A. Gómez-Pedrero, "Measurement of retardation in digital photoelasticity by load stepping using a sinusoidal least-squares fitting," *Optics and Lasers in Engineering*, vol. 41, no. 1, pp. 127–137, 2004.